ACS OMEGA

http://pubs.acs.org/journal/acsodf

Article

Efficient Cathode Buffer Material Based on Dibenzothiophene-*S*,*S*-dioxide for Both Conventional and Inverted Organic Solar Cells

Guiting Chen,*[,§] Hongli Wu,[§] Chuang Feng, Zhikai Deng, Zhuyang Li, Mingxin Nie, Baitian He,* Hongqing Hao, Xin Li, and Zhicai He*

Cite This: *ACS Omega* 2022, 7, 38613−38621

Read Online

ACCESS | Metrics & More | Article Recommendations | Supporting Information

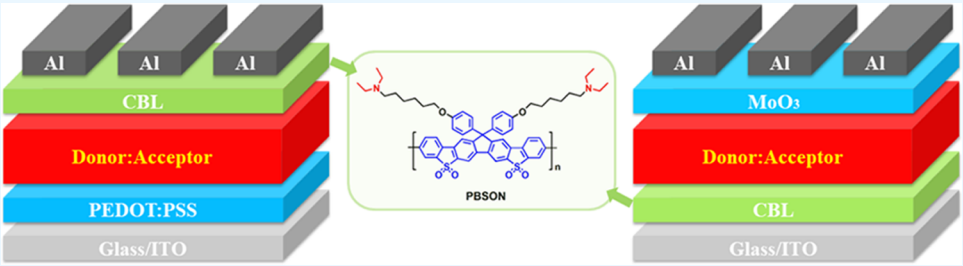

ABSTRACT: A novel conjugated molecule (PBSON) based on a main chain composed of bis(dibenzothiophene-*S*,*S*-dioxide) fused cyclopentadiene and side chains containing amino groups is presented as an efficient cathode buffer material (CBM) for organic solar cells (OSCs). PBSON showed a deep highest occupied molecular orbital (HOMO) energy level of −6.01 eV, which was beneficial for building hole-blocking layers at the cathodes of OSCs. The energy bandgap of PBSON reached 3.17 eV, implying high transmittance to visible and near-infrared light, which meant PBSON should be suitable for the applications to most inverted OSCs. The scanning Kelvin probe microscopy measurement and theoretical calculation on the PBSON/cathode interfacial interaction proved the excellent work function-regulating abilities of PBSON for various cathodes, suggesting that PBSON could promote the formation of Ohmic contacts at the cathodes and thus improve the transport and collection of electron carriers for OSCs. The characterization of electron-only devices demonstrated the good electron-transporting performance of PBSON at the cathodes. In the conventional OSCs, it was hinted that PBSON might restrain the infiltrations of evaporated cathode atoms into the active films, consequently reducing the reverse leakage currents. As a result, PBSON was able to boost the power conversion efficiencies (PCEs) by 58.2 and 56.4% for both conventional and inverted OSCs of the typical PTB7:$PC_{71}BM$ system, respectively, as compared to the unadorned devices. In terms of the classical PTB7-Th:$PC_{71}BM$ system, substantial increases in PCEs could also be found with PBSON interlayers, which were 54.7 and 59.8% for the conventional device and inverted device, respectively. Therefore, PBSON is a kind of promising CBM for realizing both conventional and inverted OSCs of high performance.

1. INTRODUCTION

Organic solar cells (OSCs) show outstanding advantages, including light weight, low cost, solution processability, and mechanical flexibility, and are becoming a kind of promising technology for the light-to-electricity conversion. In the few past decades, great efforts have been made in the engineering of active layers,[1,2] interfaces,[3] and device structures,[4] leading to the rapid improvement in power conversion efficiency (PCE), which has exceeded 18%[1−4] until now.

In conventional and inverted OSCs, the most frequently used cathodes are some metals and metal oxides with high work functions (WFs) showing excellent ambient stability, such as Al, Ag, and indium tin oxide (ITO). However, these materials are not able to form Ohmic contacts with all of the high-performance acceptors, consequently decreasing the built-in potentials (V_{bi}s) across OSCs and increasing the energy barriers of charge transportation and collection. To address the above problem, it is extremely necessary to introduce cathode buffer layers (CBLs) between the active layers and the cathodes. Efficient CBLs need to simultaneously possess many fundamental functions, such as reducing cathodes' WFs, efficiently transporting electron carriers, blocking hole carriers, reducing interfacial trap states, improving interfacial contacts, and so on.[5,6]

Received: June 29, 2022
Accepted: October 11, 2022
Published: October 21, 2022

https://doi.org/10.1021/acsomega.2c04060
ACS Omega 2022, 7, 38613−38621

The existing cathode buffer materials (CBMs) can be classified mainly as inorganic and organic species. The inorganic CBMs, including metal compounds (e.g., ZnO,[7] LiF,[8] TiO_2[9]), have been employed to improve the interfacial properties of cathodes at first. However, these materials exhibit some disadvantages, such as incompatibility with organic active films, high sensitivities toward moisture, and photocatalytic peculiarities for the degradations of active films,[10] which impede further improvements in the performance of OSCs.

In recent years, water/alcohol-soluble organic molecules (WSOMs) containing high-polarity functional groups (pyridinium salt,[5,6,11] amino,[12−14] quaternary ammonium salt,[15,16] pyridyl,[17,18] etc.) have been widely used as efficient CBMs for fabricating OSCs of high performance. With regard to these WSOMs, the general optoelectronic properties such as ultraviolet−visible (UV−vis) absorption spectra, electronic energy levels, and charge mobility usually originate from their conjugated structures. On the other hand, the cathode-modifying capabilities and water/alcohol solubility are mainly endowed by the functional groups. The water/alcohol solubility of these CBMs enables the fabrication of multilayer OSCs without interfacial corrosion via low-cost orthometric solution processing methods. The other advantages of these WSOM-based CBMs include excellent interfacial compatibility with active films, light weight, flexibility, and so on. Therefore, WSOMs are a class of indispensable materials for organic photovoltaic technologies.

Dibenzothiophene-*S*,*S*-dioxide (SO) is an efficient electron-transporting unit for photoelectric materials, which owns a relatively broad conjugated structure, high electron affinity, and excellent chemical stability.[19] Previously, some WSOMs based on SO and pyridinium salt were synthesized and used as CBMs to enhance the PCEs for OSCs successfully by us.[5,6] Moreover, we have designed and prepared a class of amino-functionalized conjugated copolymers (PBSON-P and PBSON-FEO) based on the main chains composed of bis-SO fused cyclopentadiene (BSO) and benzene or fluorene.[20] The novel aromatic systems offered these WSOMs with interesting properties such as efficient electron-transporting and hole-blocking performance when PBSON-P and PBSON-FEO were employed as CBMs to OSCs. As a result, simultaneous improvements in the open-circuit voltage (V_{oc}), fill factor (FF), and PCE could be realized, suggesting the great potential of BSO units to develop high-efficiency CBMs.

In this work, to further investigate the intrinsic cathode-buffering properties of the BSO building block, a novel conjugated molecule named PBSON based on a repeating unit of amino-modified BSO was presented. It was found that PBSON showed a deeper highest occupied molecular orbital (HOMO) energy level (E_{HOMO}) of −6.01 eV as compared to the corresponding copolymers,[20] offering efficient hole-blocking performance for the cathodes. The energy bandgap (E_g) of PBSON was enlarged to 3.17 eV, indicating the high transmittance to visible and near-infrared light of CBLs, which should be able to maintain the light absorption of active layers in the inverted devices. The scanning Kelvin probe microscopy (SKPM) measurement and theoretical calculation on an interfacial model verified the prominent WF-regulating abilities of PBSON for cathodes endowed by the amino groups, signifying that PBSON could help form Ohmic contacts at the cathodes and thus improve the electron-transporting and -collecting performance for OSCs. Besides, the characterization of electron-only devices further demonstrated the good electron-transporting performance of PBSON at the cathodes. When PBSON was used as a CBM to the classical OSCs of poly[4,8-bis(2-ethylhexyloxyl)benzo[1,2-*b*;4,5-*b*′]dithiophene-2,6-diyl-*alt*-(4-(2-ethylhexyl)-3-fluorothieno[3,4-*b*]thiophene-2-carboxylate-2,6-diyl)] (PTB7):[6,6]-phenyl C_{71}-butyric acid methyl ester ($PC_{71}BM$), it was found to enhance PCEs by 58.2 and 56.4% for the conventional and inverted devices, respectively, in comparison to OSCs with unmodified cathodes. In the matter of poly[4,8-bis(5-(2-ethylhexyl)thiophen-2-yl)benzo[1,2-*b*;4,5-*b*′]-dithiophene-2,6-diyl-*alt*-(4-(2-ethylhexyl)-3-fluorothieno[3,4-*b*]thiophene-2-carboxylate-2,6-diyl)] (PTB7-Th):$PC_{71}BM$-based OSCs, PBSON exhibited outstanding cathode-modifying properties as well, and the PCE was increased by 54.7% for the conventional device and 59.8% for the inverted one.

2. RESULTS AND DISCUSSION

2.1. Synthesis and Characterization. The molecular structure of PBSON is shown in Chart 1, and the corresponding synthetic route and procedures are displayed in the Supporting Information. Monomer **1** was prepared according to the previously reported method by us.[20] Then, the common Pd-catalyzed Stille coupling reaction between monomer **1** and hexabutylditin (**2**) generated PBSON successfully. PBSON showed a number average molecular weight (M_n) of about 6900 and a polydispersity of 1.3, estimated on gel permeation chromatography (GPC). The relatively small M_n might be attributed to the relatively low solubility of the polymeric intermediate in the reactive solvent system composed of toluene and *N*,*N*-dimethylformamide, as some precipitate could be observed during the polymerization. PBSON was soluble in the common moderately polar organic solvents such as tetrahydrofuran (THF) and $CHCl_3$, and also could be dissolved in the mixed solvent composed of MeOH and trace trifluoroacetic acid (TFA) (with a volume fraction of 0.5%) due to the ionized reaction between the amino groups and TFA. It was found that the solvent system of MeOH containing trace HOAc, which is often used to process the amino-functionalized CBLs,[12] was unable to solubilize PBSON, probably because a stronger ionized conversion of amino groups was required for PBSON with a big conjugated structure to be dissolved in MeOH. In a word, multilayer OSCs can be fabricated via the low-temperature orthometric solution processing technology when employing this new molecule as a CBM.

Chart 1. Molecular Structure of PBSON

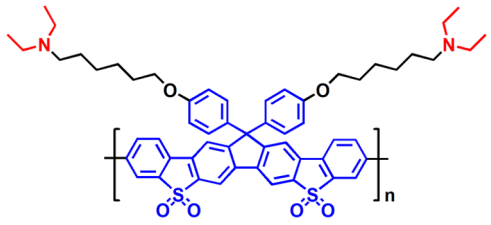

PBSON

2.2. Photophysical Properties. The UV−vis absorption and photoluminescence (PL) spectra of PBSON in the dilute CH_2Cl_2 solution and in the film are shown in Figure 1a, and the corresponding parameters are summarized in Table 1. In the CH_2Cl_2 solution, PBSON displayed two spiculate

https://doi.org/10.1021/acsomega.2c04060
ACS Omega 2022, 7, 38613−38621

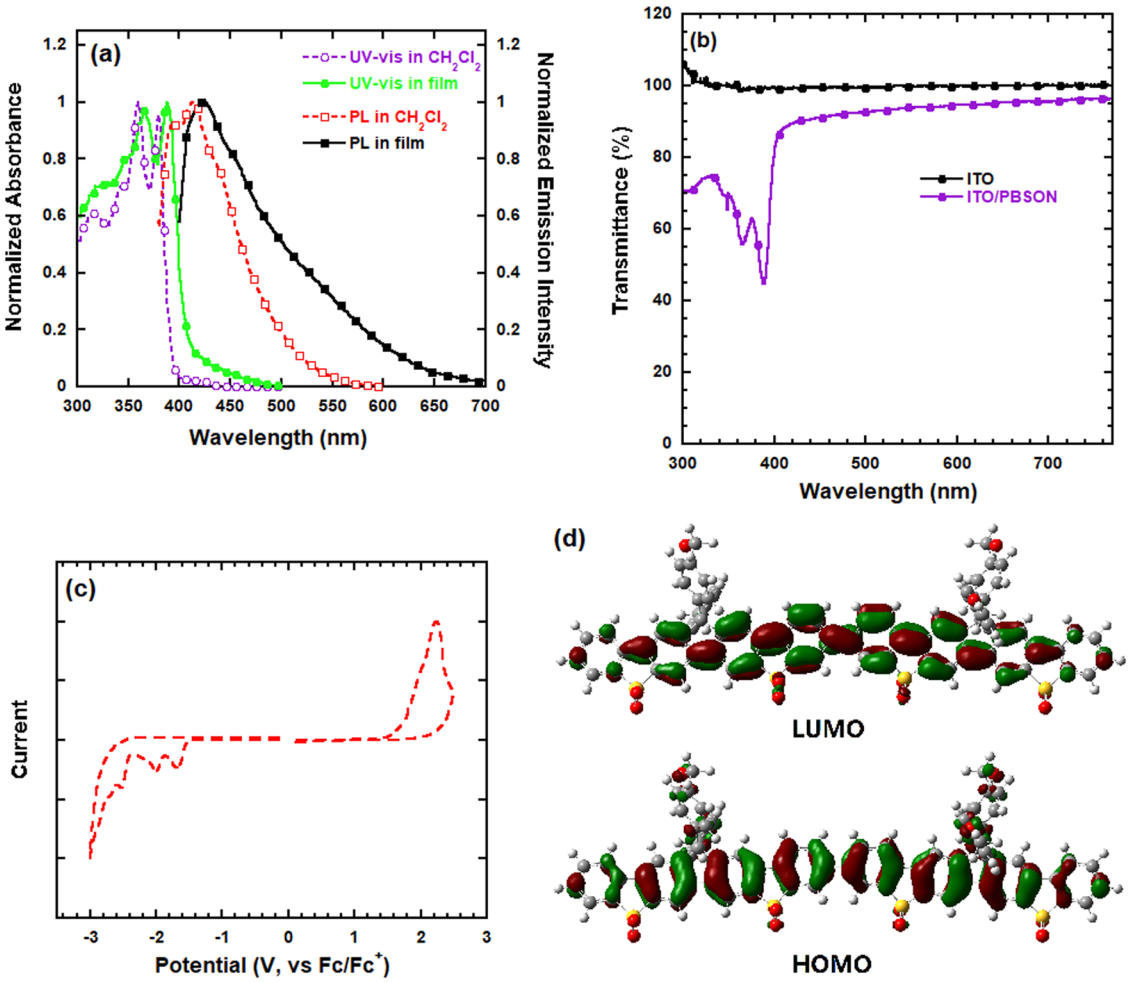

Figure 1. (a) UV−vis absorption and PL spectra, (b) optical transmission spectrum in the film, (c) CV curve in the film, and (d) DFT calculated FMOs of the methoxy-substituted dimer of the repeating unit of PBSON.

Table 1. Photophysical and Electrochemical Parameters of PBSON

	CH_2Cl_2		film					
molecule	λ_{abs} (nm)	λ_{PL} (nm)	λ_{abs} (nm)	λ_{PL} (nm)	E_g^{opt} (eV)	E_{HOMO} (eV)	E_{LUMO} (eV)	E_g^e (eV)
PBSON	358, 380	413	365, 388	424	3.05	−6.01	−2.84	3.17

absorption peaks at 358 and 380 nm. These correlative signals exhibited bathochromic shifts to 365 and 388 nm in the film state due to the intermolecular $\pi-\pi$ aggregation effect. The optical E_g (E_g^{opt}) could be calculated as 3.05 eV from the absorption edge in the film. As for the PL properties, the emitting peaks were located at 413 and 424 nm in the solution and in the film, respectively, suggesting blue light emission for PBSON.

The optical transmission spectrum of PBSON in the film is presented in Figure 1b. The processing condition of the PBSON film here was the same as that in the inverted OSCs, as discussed later. The ITO substrate showed extremely high transmittance in the wavelength range higher than 300 nm. For the ITO/PBSON substrate, the transmittance profile in the wavelength range of 300−410 nm matched well with the corresponding absorption curve in the film. The transmittance values exceeded 90% in the wavelength range higher than 425 nm, signifying excellent visible and near-infrared light transparency of PBSON.

2.3. Electrochemical Properties and Theoretical Calculations. The electrochemical properties of PBSON were investigated, and the resulting cyclic voltammetry (CV) curve is exhibited in Figure 1c. In the CV profile of PBSON, the onset potentials of oxidation (E_{ox}) and reduction (E_{red}) were 1.66 and −1.51 V, respectively. Besides, the oxidation potential of ferrocene/ferrocenium (Fc/Fc^+) against the reference electrode of saturated calomel was measured as 0.45 V. Therefore, the E_{HOMO} and lowest unoccupied molecular orbital (LUMO) energy level (E_{LUMO}) of PBSON could be evaluated from the empirical equations of $E_{HOMO} = -(4.80 + E_{ox} - 0.45)$ eV and $E_{LUMO} = -(4.80 + E_{red} - 0.45)$ eV,[21] and the values were −6.01 and −2.84 eV, respectively. Consequently, the electrochemical E_g (E_g^e) was calculated to be 3.17 eV, as shown in Table 1.

To get an insightful understanding of the optimal molecular geometry and electronic properties of PBSON, a density functional theory (DFT) calculation at the B3LYP level with the 6-31G* basis set was performed for the dimer of the repeating unit, during which the side chains were replaced with

https://doi.org/10.1021/acsomega.2c04060
ACS Omega 2022, 7, 38613−38621

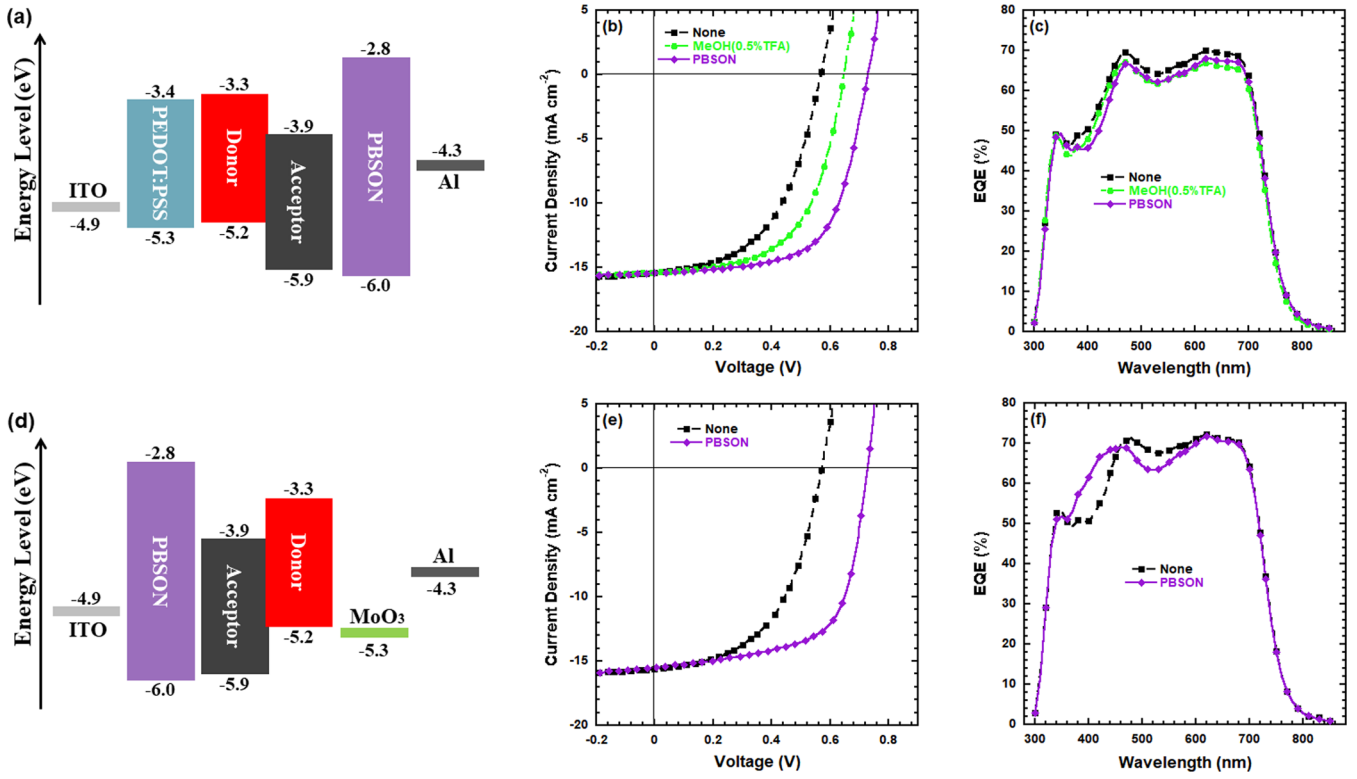

Figure 2. Energy level diagrams, $J-V$ characteristic curves under AM 1.5G irradiation, and EQE spectra of conventional (a–c) and inverted (d–f) PTB7:$PC_{71}BM$ OSCs subjected to different cathode treatments.

Table 2. Photovoltaic Parameters under AM 1.5G Irradiation of Conventional and Inverted PTB7:$PC_{71}BM$ OSCs Subjected to Different Cathode Treatments

OSCs structure	CBL	V_{oc} (V)	J_{sc} (mA cm^{-2})	FF (%)	PCE (%)
conventional	none	0.57[a](0.57)[b]	15.39(15.30)	51.51(51.28)	4.52(4.47)
	MeOH(0.5%TFA)	0.65(0.65)	15.41(15.22)	57.44(57.16)	5.75(5.65)
	PBSON	0.73(0.73)	15.44(15.28)	63.43(63.31)	7.15(7.06)
inverted	none	0.57(0.57)	15.65(15.53)	52.25(52.07)	4.66(4.61)
	PBSON	0.73(0.73)	15.50(15.29)	64.41(64.24)	7.29(7.17)

[a]Values from the best devices. [b]Average values calculated from three devices.

Table 3. WFs of Various Cathodes Subjected to Different Treatments

	WF (eV)	
CBL	Ag	ITO
none	4.73	4.70
PBSON	4.18	4.58

methoxy groups to simplify the computation.[22] The optimized molecular geometry is shown in Figure S1 (see the Supporting Information), and the calculated frontier molecular orbitals (FMOs) are displayed in Figure 1d. The conjugated main chain of this molecule exhibited nonplanar conformation at the lower state due to torsional strains between those neighboring aromatic rings, and both the HOMO and LUMO were delocalized mainly over the conjugated main chain barring the phenyl side chains. The calculated E_{HOMO} and E_{LUMO} were −5.97 and −2.55 eV, respectively.

2.4. Photovoltaic Performance. To study the cathode-buffering performance of PBSON for OSCs, both the conventional and inverted devices based on the PTB7:$PC_{71}BM$ system were fabricated and measured. The energy level diagrams, current density-voltage ($J-V$) curves under AM 1.5G irradiation, and external quantum efficiency (EQE) spectra of these OSCs are shown in Figure 2, and the extracted photovoltaic parameters are summarized in Table 2. As for the conventional device without any cathode treatment, the V_{oc}, short-circuit current density (J_{sc}), FF, and PCE were 0.57 V, 15.39 mA cm^{-2}, 51.51 and 4.52%, respectively. When MeOH containing 0.5% TFA was used to wash the active film, the aforementioned parameters were changed to 0.65 V, 15.41 mA cm^{-2}, 57.44 and 5.75%, respectively. It is worth noting that when a thin layer of PBSON was inserted between the active layer and cathode, the PCE was increased to 7.15%, accompanied by the V_{oc} at 0.73 V, J_{sc} at 15.44 mA cm^{-2}, and FF at 63.43%. It was found that the significant improvement in PCE by PBSON was mainly attributed to the enhancements in the V_{oc} and FF. On the other hand, it can be seen that the modified device showed slightly lower EQE values than the pristine one, as shown in Figure 2c, which might be due to the higher light transmittance of the cathode substrate for the pristine device. However, these OSCs exhibited close J_{sc}s, probably resulting from that the untreated device owned nonideal energy level alignment (as discussed in

https://doi.org/10.1021/acsomega.2c04060
ACS Omega 2022, 7, 38613−38621

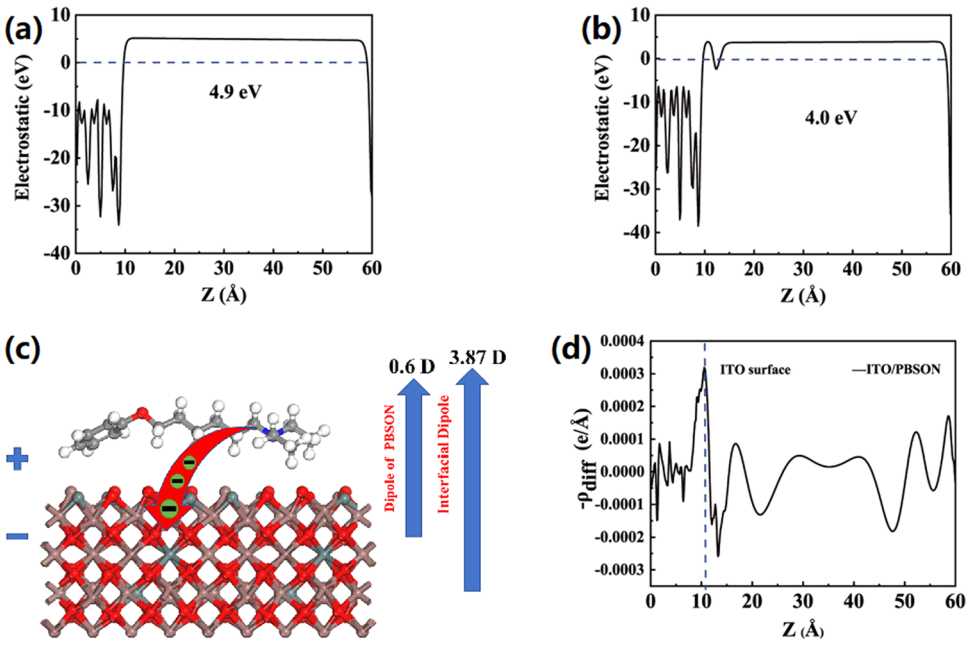

Figure 3. Calculated WFs of (a) ITO and (b) ITO/PBSON, (c) the proposed forming mechanism diagram of dipoles at the ITO/PBSON interface, and (d) electron density differences along the surface normal (z) averaged over the xy plane in units of Å^{-3} of PBSON on the surface of ITO.

the following WFs test) and thus poor charge carrier-transporting ability at the cathode. Therefore, although the EQEs were higher (due to the higher light absorption), the light current could not be converted efficiently for the unmodified device. This could also be proven by the lower FF and electron mobility (see the following electron-only devices test) for the pristine device.

In regard to the inverted unadorned OSC, the photovoltaic parameters were 0.57 V, 15.65 mA cm^{-2}, 52.25 and 4.66% for the V_{oc}, J_{sc}, FF, and PCE, respectively. However, the PBSON-modified device showed evident performance improvement as well, with the V_{oc} at 0.73 V, J_{sc} at 15.50 mA cm^{-2}, FF at 64.41%, and PCE at 7.29%. Apparently, the V_{oc} and FF increases resulted in the PCE improvement, which was similar to the conventional devices. The EQE spectra are shown in Figure 2f, in which the PBSON-modified device displayed higher EQEs in the short-wavelength region and lower EQEs in the long-wavelength region as compared to the pristine device. This change in the EQE profile might be attributed to the changes in optical parameters (refractive index, extinction coefficient, etc.) of the functional layers, leading to the variation in optical field distribution when inserting PBSON into the device.[23]

Moreover, the conventional OSCs based on an ITO/PEDOT:PSS/PTB7-Th:$PC_{71}BM$/CBL/Al structure and inverted OSCs based on an ITO/CBL/PTB7-Th:$PC_{71}BM$/MoO_3/Al structure were also prepared and tested. The J−V curves under AM 1.5G irradiation of these OSCs are shown in Figure S2, and the corresponding photovoltaic parameters are displayed in Table S1. The PCE of the conventional device was increased from 5.23% (V_{oc} = 0.58 V, J_{sc} = 16.46 mA cm^{-2}, FF = 54.77%) to 6.38% (V_{oc} = 0.66 V, J_{sc} = 16.47 mA cm^{-2}, FF = 58.70%) when the solvent was used to wash the active layer. However, the PCE could be enhanced to 8.09% (V_{oc} = 0.77 V, J_{sc} = 16.51 mA cm^{-2}, FF = 63.64%) for the device subjected to PBSON modification. On the other hand, the inverted device was able to realize PCE improvement from 5.10% (V_{oc} = 0.58 V, J_{sc} = 16.29 mA cm^{-2}, FF = 54.01%) to 8.15% (V_{oc} = 0.77 V, J_{sc} = 16.38 mA cm^{-2}, FF = 64.59%) when inserting a PBSON interlayer. Hence, PBSON is a kind of high-efficiency CBM which can boost the performance of different OSCs significantly.

2.5. WF Properties of Cathodes. To explore the working mechanisms of PBSON, the regulating abilities of PBSON for the WFs of cathodes were tested on a SKPM, as shown in Table 3. As for the pure Ag electrode, the WF was measured to be 4.73 eV; however, when the surface of Ag was coated with a PBSON thin film, the WF was decreased to 4.18 eV by a large margin. A similar result could be observed with the ITO samples, which showed a WF reduction from 4.70 to 4.58 eV when spin-coating a PBSON thin film on the ITO substrate. The mechanism for changes in WF was speculated to be the formation of directed dipoles at the active film/cathode interfaces induced by PBSON.[12] The decreased WFs of cathodes could enlarge the V_{bi}s across the OSCs, which enhanced the V_{oc}s finally.

To further study the interfacial interactions between PBSON and cathodes, we established a molecular model of PBSON on the surface of ITO.[24] The cathode-modifying effects of organic CBLs containing high-polarity functional groups for OSCs have been proposed to originate from the influences of functional groups, such as the amino group and phosphonic acid group.[25] As a typical example, the amino groups of PFN interlayers dominate the interfacial interactions and formations of interfacial dipoles in OSCs.[24] Therefore, it should be reasonable to examine the interfacial interaction dynamic between the amino-inlayed side chain of the PBSON and cathode such as ITO. In the theoretical calculation, when PBSON was adsorbed on the surface of ITO, the WF of ITO was decreased from 4.9 to 4.0 eV, as shown in Figure 3a,b. The variation of WFs was equivalent to an interfacial dipole of 3.87 D, and the direction of the dipole was from ITO to PBSON, as shown in Figure 3c. Moreover, the vertical component of the dipole of this molecule itself was calculated as 0.6 D, as

https://doi.org/10.1021/acsomega.2c04060
ACS Omega 2022, 7, 38613−38621

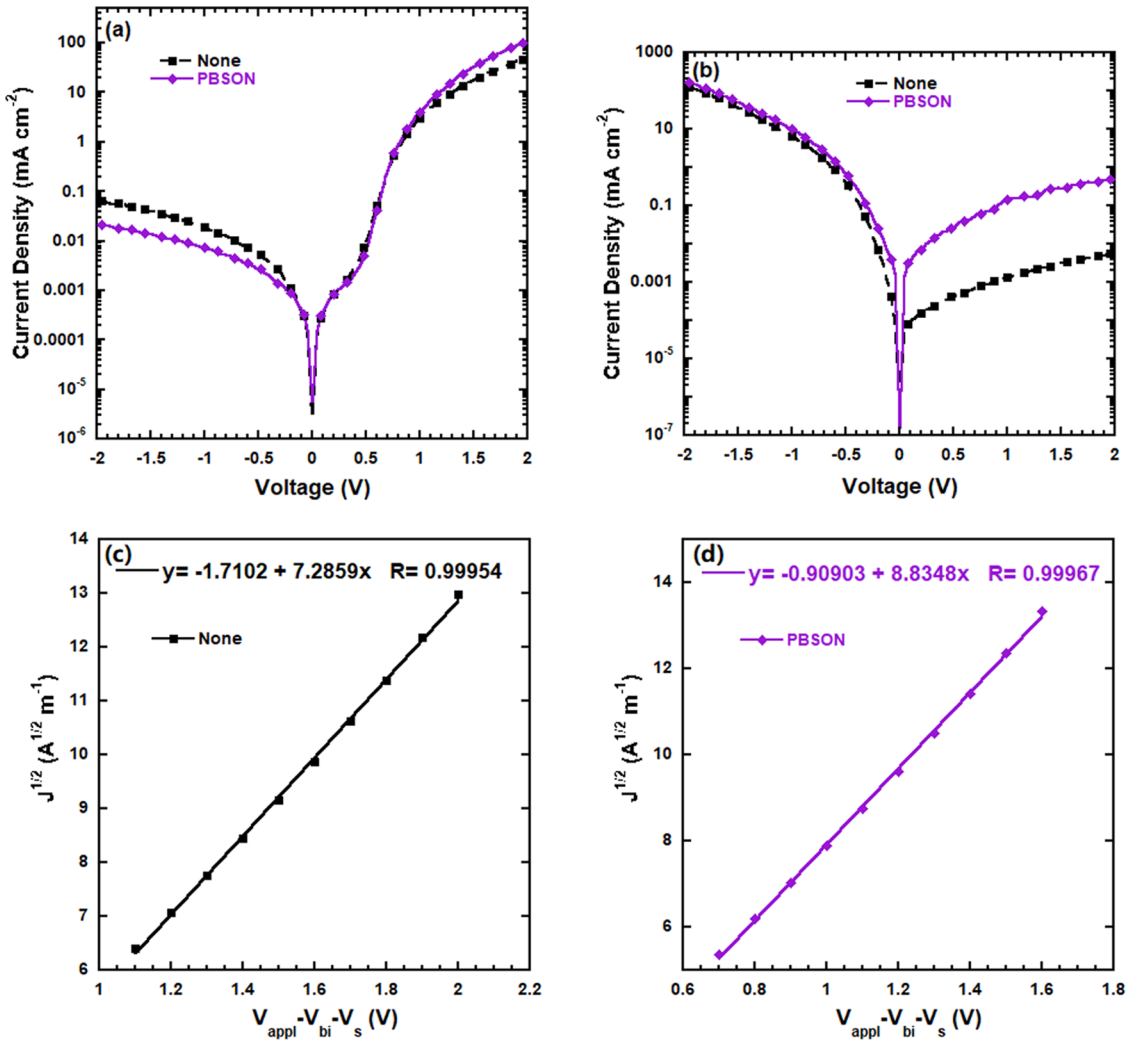

Figure 4. J–V characteristic curves of (a) conventional and (b) inverted PTB7:$PC_{71}BM$ OSCs subjected to different cathode treatments in the dark, and (c, d) fitting curves with the SCLC model of PTB7:$PC_{71}BM$ electron-only devices subjected to different cathode treatments.

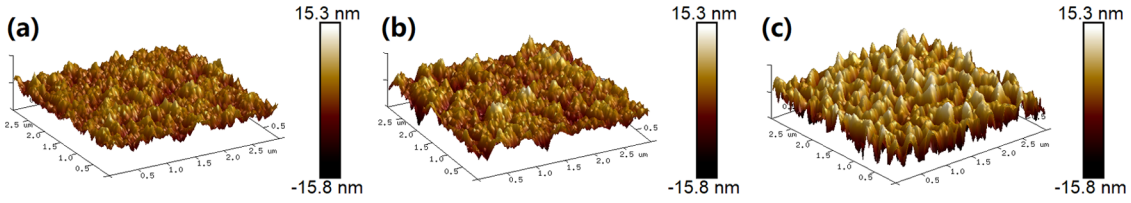

Figure 5. 3D surface topographic images (size: 3 μm × 3 μm) of (a) pristine, (b) MeOH (with 0.5% TFA)-treated, and (c) PBSON-coated PTB7:$PC_{71}BM$ films.

presented in Figure 3c. It could be inferred that the dipole induced by the charge transfer from the amino group to ITO was 3.27 D, and the direction was also from ITO to PBSON. Hence, these two dipoles could be superposed when PBSON was adsorbed on the surface of ITO, leading to a decrease in the ITO WF. In addition, the electron density differences of PBSON on the surface of ITO were also calculated, as shown in Figure 3d. The result suggested that there was an obvious electron transfer from PBSON to ITO, which further proved the formation of the interfacial dipole, and the direction was from ITO to PBSON.

2.6. *J*–*V* Curves in the Dark. The J–V characteristic curves in the dark of conventional and inverted PTB7:$PC_{71}BM$ OSCs were recorded, as shown in Figure 4a,b. As for the conventional device, it could be seen that the reverse dark J values were obviously restrained when introducing a PBSON layer. It has been reported that the J values in this region depend mainly on the qualities and thicknesses of active films; hence, the decreases in the reverse leakage J might benefit from that PBSON generated a protective layer to prevent the evaporated cathode atoms from infiltrating into the active film.[26] Moreover, the J values of the PBSON-treated conventional device were distinctly higher than those of the unadorned one in the forward high-bias area, which could be observed in the inverted OSCs as well, meaning the improved electron injections and transports of cathodes when inserting PBSON CBLs.[26] This might be attributed to the formation of Ohmic contacts between the acceptors and cathodes induced

https://doi.org/10.1021/acsomega.2c04060
ACS Omega 2022, 7, 38613−38621

by the WF-adjusting abilities of PBSON for cathodes and to the good electron-transporting capabilities of PBSON at the cathodes, as discussed below.

The series resistance (R_s) calculated from the forward high-bias area of the $J-V$ curve in the dark[27] was reduced from 36.9 to 15.4 Ω cm^2 when employing a PBSON interlayer into the conventional device. Besides, as compared to the inverted device with an unmodified cathode showing a R_s at 11.7 Ω cm^2, a smaller R_s at 8.81 Ω cm^2 could also be found in the modified one. This implied that PBSON interlayers could improve the interfacial contacts and charge carrier-transporting performance of cathodes, which was consistent with the enhanced FFs of both conventional and inverted OSCs with PBSON interlayers.

2.7. Electron-Only Devices. To investigate the electron-transporting performance of PBSON thoroughly, electron-only devices with a structure of ITO/ZnO/PTB7:$PC_{71}BM$/CBL/Ag were fabricated and tested, and the results were fitted with the space−charge−limited current (SCLC) model,[28] as shown in Figure 4c,d. The active layers and CBL were processed in the same way as the conventional OSCs. The device without any cathode treatment showed an apparent electron mobility of 6.09×10^{-6} cm^2 V^{-1} s^{-1}. Interestingly, the electron mobility was enhanced to 1.60×10^{-5} cm^2 V^{-1} s^{-1} when introducing a PBSON layer into the cathode. The good charge carrier-transporting performance of this molecule, suggested by the increased mobility, could be responsible for the improvements in the FF and PCE of OSCs.

2.8. Topographies. Atomic force microscopy (AFM) was used to study the topographies of PTB7:$PC_{71}BM$ active films subjected to different treatments, and the three-dimensional (3D) images are displayed in Figure 5. The unadorned PTB7:$PC_{71}BM$ film exhibited a smooth surface with a root-mean-square roughness (R_q) at 2.45 nm. The active film became slightly rougher with a R_q of 2.91 nm after washing with MeOH (containing 0.5% TFA). However, the topography turned into a lumpy surface showing a R_q at 5.28 nm when a PBSON thin film was deposited on top, which might be due to the rigid molecular structure and mediocre film-forming property of PBSON. The rough CBL could generate large contact areas with the top metal cathodes, which might be helpful to the electron extraction to the cathodes and thus FF improvements, agreeing with the previous reports.[29,30]

3. CONCLUSIONS

In summary, a novel conjugated molecule named PBSON based on a repeating unit of amino-functionalized BSO was designed and synthesized. It was proved that the PBSON CBM could boost the PCEs by 58.2 and 56.4% for the conventional and inverted OSCs of PTB7:$PC_{71}BM$, respectively. As for the PTB7-Th:$PC_{71}BM$-based OSCs, PBSON was able to increase the PCEs by 54.7% for the conventional device and 59.8% for the inverted one. The improvements in PCE for the above OSCs resulted mainly from the synchronous enhancements in the V_{oc} and FF. PBSON exhibited a deep E_{HOMO} of −6.01 eV and a large E_g^e of 3.17 eV, implying effective hole-blocking properties and favorable applications to inverted devices, respectively. The SKPM measurement and theoretical calculation on an interfacial model verified that PBSON showed excellent WF-regulating abilities for cathodes, which promoted the formation of Ohmic contacts at the cathodes and the V_{bi} and V_{oc} enhancements of OSCs. In the conventional OSCs, PBSON might prevent the evaporated cathode atoms from diffusing into the active films, consequently reducing the reverse leakage currents, which could be hinted from the $J-V$ curves of OSCs in the dark. Moreover, it was suggested from the measurement of electron-only devices that PBSON displayed good electron-transporting capabilities and was able to improve the charge carrier transport of cathodes, giving rise to enlargements in the FF. Therefore, PBSON is a promising CBM which can improve the performance of both conventional and inverted OSCs efficiently.

4. EXPERIMENTAL SECTION

All of the relevant materials, reagents, and solvents were purchased from Energy Chemical Co., Aladdin Chemical Co., and Sigma Aldrich Chemical Co. and were used directly without further purification. The solvents used in the moisture-sensitive reactions and tests were further dried by the general procedures and distilled before use. The synthetic route and procedures, chemical characterizations, and fabrications and characterizations of OSCs are presented in the Supporting Information.

■ ASSOCIATED CONTENT

Supporting Information

The Supporting Information is available free of charge at https://pubs.acs.org/doi/10.1021/acsomega.2c04060.

Experimental section including the procedures and methods of synthesis and characterizations of the molecule and fabrications and measurements of OSCs; DFT-optimized molecular geometry of the PBSON model; and photovoltaic performance of PTB7-Th/$PC_{71}BM$-based OSCs (PDF)

■ AUTHOR INFORMATION

Corresponding Authors

Guiting Chen − *School of Chemistry and Environment, Jiaying University, Meizhou 514015, China;* orcid.org/0000-0002-5451-1485; Email: cgt_jy@126.com

Baitian He − *School of Chemistry and Environment, Jiaying University, Meizhou 514015, China*; Email: baitian-he@foxmail.com

Zhicai He − *Institute of Polymer Optoelectronic Materials and Devices, State Key Laboratory of Luminescent Materials and Devices, South China University of Technology, Guangzhou 510640, China;* orcid.org/0000-0003-0164-8645; Email: zhicaihe@scut.edu.cn

Authors

Hongli Wu − *Institute of Polymer Optoelectronic Materials and Devices, State Key Laboratory of Luminescent Materials and Devices, South China University of Technology, Guangzhou 510640, China*

Chuang Feng − *Institute of Polymer Optoelectronic Materials and Devices, State Key Laboratory of Luminescent Materials and Devices, South China University of Technology, Guangzhou 510640, China*

Zhikai Deng − *School of Chemistry and Environment, Jiaying University, Meizhou 514015, China*

Zhuyang Li − *School of Chemistry and Environment, Jiaying University, Meizhou 514015, China*

Mingxin Nie − *School of Chemistry and Environment, Jiaying University, Meizhou 514015, China*

https://doi.org/10.1021/acsomega.2c04060
ACS Omega 2022, 7, 38613−38621

Hongqing Hao − *School of Chemistry and Environment, Jiaying University, Meizhou 514015, China*
Xin Li − *School of Chemistry and Environment, Jiaying University, Meizhou 514015, China*

Complete contact information is available at: https://pubs.acs.org/10.1021/acsomega.2c04060

Author Contributions

§G.C. and H.W. contributed equally to this work. The manuscript was written through contributions of all authors. All authors have given approval to the final version of the manuscript.

Notes

The authors declare no competing financial interest.

■ ACKNOWLEDGMENTS

This work was financially supported by the Guangdong Basic and Applied Basic Research Foundation (2019A1515011141), the Innovation and Entrepreneurship Training Program for Undergraduates (621A0255), the Guangdong International Science and Technology Cooperation Foundation (2020A0505100002), and the Guangdong-Hong Kong-Macao Joint Laboratory of Optoelectronic and Magnetic Functional Materials (2019B121205002).

■ REFERENCES

(1) Bao, S.; Yang, H.; Fan, H.; Zhang, J.; Wei, Z.; Cui, C.; Li, Y. Volatilizable solid additive-assisted treatment enables organic solar cells with efficiency over 18.8% and fill factor exceeding 80%. *Adv. Mater.* **2021**, *33*, No. 2105301.
(2) Liu, Q.; Jiang, Y.; Jin, K.; Qin, J.; Xu, J.; Li, W.; Xiong, J.; Liu, J.; Xiao, Z.; Sun, K.; Yang, S.; Zhang, X.; Ding, L. 18% Efficiency organic solar cells. *Sci. Bull.* **2020**, *65*, 272−275.
(3) Liu, L.; Chen, S.; Qu, Y.; Gao, X.; Han, L.; Lin, Z.; Yang, L.; Wang, W.; Zheng, N.; Liang, Y.; Tan, Y.; Xia, H.; He, F. Nanographene-osmapentalyne complexes as a cathode interlayer in organic solar cells enhance efficiency over 18%. *Adv. Mater.* **2021**, *33*, No. 2101279.
(4) Hong, L.; Yao, H.; Cui, Y.; Bi, P.; Zhang, T.; Cheng, Y.; Zu, Y.; Qin, J.; Yu, R.; Ge, Z.; Hou, J. 18.5% Efficiency organic solar cells with a hybrid planar/bulk heterojunction. *Adv. Mater.* **2021**, *33*, No. 2103091.
(5) Chen, G.; Liu, S.; Xu, J.; He, R.; He, Z.; Wu, H.-B.; Yang, W.; Zhang, B.; Cao, Y. Dibenzothiophene-*S*,*S*-dioxide and bispyridinium-based cationic polyfluorene derivative as an efficient cathode modifier for polymer solar cells. *ACS Appl. Mater. Interfaces* **2017**, *9*, 4778−4787.
(6) Chen, G.; Cheng, D.; Zou, W.; Cai, Z.; Xie, Y.; Chen, Y.; He, B.; Hao, H.; Yang, W.; Cao, Y. Dibenzothiophene-*S*,*S*-dioxide-bispyridinium-fluorene-based polyelectrolytes for cathode buffer layers of polymer solar cells. *Polym. Chem.* **2020**, *11*, 3605−3614.
(7) Hau, S.-K.; Yip, H.; Baek, N. S.; Zou, J.; O'Malley, K.; Jen, A. K.-Y. Air-stable inverted flexible polymer solar cells using zinc oxide nanoparticles as an electron selective layer. *Appl. Phys. Lett.* **2008**, *92*, No. 253301.
(8) Brabec, C. J.; Shaheen, S. E.; Winder, C.; Sariciftci, N. S.; Denk, P. Effect of LiF/metal electrodes on the performance of plastic solar cells. *Appl. Phys. Lett.* **2002**, *80*, 1288−1290.
(9) Hayakawa, A.; Yoshikawa, O.; Fujieda, T.; Uehara, K.; Yoshikawa, S. High performance polythiophene/fullerene bulk-heterojunction solar cell with a TiO_x hole blocking layer. *Appl. Phys. Lett.* **2007**, *90*, No. 163517.
(10) Park, S.; Son, H. J. Intrinsic photo-degradation and mechanism of polymer solar cells: the crucial role of non-fullerene acceptors. *J. Mater. Chem. A* **2019**, *7*, 25830−25837.
(11) Chen, G.; Liu, S.; He, Z.; Wu, H.-B.; Yang, W.; Zhang, B. Efficient interface engineering enhances photovoltaic performance of a bulk-heterojunction PCDTBT:$PC_{71}BM$ system. *IEEE J. Photovoltaics* **2019**, *9*, 1258−1265.
(12) He, Z.; Zhong, C.; Huang, X.; Wong, W.-Y.; Wu, H.-B.; Chen, L.; Su, S.; Cao, Y. Simultaneous enhancements of open-circuit voltage, short-circuit current density, and fill factor in polymer solar cells. *Adv. Mater.* **2011**, *23*, 4636−4643.
(13) Yao, J.; Qiu, B.; Zhang, Z.-G.; Xue, L.; Wang, R.; Zhang, C.; Chen, S.; Zhou, Q.; Sun, C.; Yang, C.; Xiao, M.; Meng, L.; Li, Y. Cathode engineering with perylene-diimide interlayer enabling over 17% efficiency single-junction organic solar cells. *Nat. Commun.* **2020**, *11*, No. 2726.
(14) Zhang, Z.-G.; Qi, B.; Jin, Z.; Chi, D.; Qi, Z.; Li, Y.; Wang, J. Perylene diimides: a thickness-insensitive cathode interlayer for high performance polymer solar cells. *Energy Environ. Sci.* **2014**, *7*, 1966−1973.
(15) Wu, Z.; Sun, C.; Dong, S.; Jiang, X.-F.; Wu, S.; Wu, H.-B.; Yip, H.-L.; Huang, F.; Cao, Y. n-Type water/alcohol-soluble naphthalene diimide-based conjugated polymers for high-performance polymer solar cells. *J. Am. Chem. Soc.* **2016**, *138*, 2004−2013.
(16) Cai, C.; Yao, J.; Chen, L.; Yuan, Z.; Zhang, Z.-G.; Hu, Y.; Zhao, X.; Zhang, Y.; Chen, Y.; Li, Y. Silicon naphthalocyanine tetraimides: cathode interlayer materials for highly efficient organic solar cells. *Angew. Chem., Int. Ed.* **2021**, *60*, 19053−19057.
(17) Chen, G.; Liu, S.; He, Z.; Wu, H.-B.; Yang, W.; Zhang, B.; Cao, Y. Pyridine-incorporated alcohol-soluble neutral polyfluorene derivatives as efficient cathode-modifying layers for polymer solar cells. *Polym. Chem.* **2017**, *8*, 6720−6732.
(18) Lin, L.; Huang, Z.; Luo, Y.; Peng, T.; He, B.; Chen, G.; Hao, H.; Li, X.; Cai, P.; Yang, W. Alcohol-soluble fluorene derivate functionalized with pyridyl groups as a high-performance cathode interfacial material in organic solar cells. *New J. Chem.* **2021**, *45*, 4584−4591.
(19) He, R.-F.; Xu, J.; Xue, Y.; Chen, D.-C.; Ying, L.; Yang, W.; Cao, Y. Improving the efficiency and spectral stability of white-emitting polycarbazoles by introducing a dibenzothiophene-*S*,*S*-dioxide unit into the backbone. *J. Mater. Chem. C* **2014**, *2*, 7881−7890.
(20) Chen, G.; Qian, G.; Yi, S.; He, Z.; Wu, H.-B.; Yang, W.; Zhang, B.; Cao, Y. Molecular engineering on bis(benzothiophene-*S*,*S*-dioxide)-based large-band gap polymers for interfacial modifications in polymer solar cells. *ACS Appl. Mater. Interfaces* **2019**, *11*, 45969−45978.
(21) Pommerehne, J.; Vestweber, H.; Guss, W.; Mahrt, R. F.; Bassler, H.; Porsch, M.; Daub, J. Efficient two layer LEDs on a polymer blend basis. *Adv. Mater.* **1995**, *7*, 551−554.
(22) Becke, A. D. Density-functional thermochemistry. III. The role of exact exchange. *J. Chem. Phys.* **1993**, *98*, 5648−5652.
(23) He, Z.; Zhong, C.; Su, S.; Xu, M.; Wu, H.-B.; Cao, Y. Enhanced power-conversion efficiency in polymer solar cells using an inverted device structure. *Nat. Photonics* **2012**, *6*, 591−595.
(24) Feng, C.; Wang, X.; He, Z.; Cao, Y. Formation mechanism of PFN dipole interlayer in organic solar cells. *Solar RRL* **2021**, *5*, No. 2000753.
(25) Timpel, M.; Li, H.; Nardi, M. V.; Wegner, B.; Frisch, J.; Hotchkiss, P. J.; Marder, S. R.; Barlow, S.; Brédas, J.-L.; Koch, N. Electrode work function engineering with phosphonic acid monolayers and molecular acceptors: charge redistribution mechanisms. *Adv. Funct. Mater.* **2018**, *28*, No. 1704438.
(26) Zhang, F.; Ceder, M.; Inganäs, O. Enhancing the photovoltage of polymer solar cells by using a modified cathode. *Adv. Mater.* **2007**, *19*, 1835−1838.
(27) Yakuphanoglu, F. Photovoltaic properties of the organic-inorganic photodiode based on polymer and fullerene blend for optical sensors. *Sens. Actuators, A* **2008**, *141*, 383−389.
(28) Murgatroyd, P. N. Theory of space-charge-limited current enhanced by Frenkel effect. *J. Phys. D: Appl. Phys.* **1970**, *3*, 151−156.
(29) Chen, D.; Zhou, H.; Liu, M.; Zhao, W.-M.; Su, S.-J.; Cao, Y. Novel cathode interlayers based on neutral alcohol-soluble small

molecules with a triphenylamine core featuring polar phosphonate side chains for high-performance polymer light-emitting and photovoltaic devices. *Macromol. Rapid Commun.* **2013**, *34*, 595−603.
(30) Ye, H.; Hu, X.-W.; Jiang, Z.-X.; Chen, D.-C.; Liu, X.; Nie, H.; Su, S.-J.; Gong, X.; Cao, Y. Pyridinium salt-based molecules as cathode interlayers for enhanced performance in polymer solar cells. *J. Mater. Chem. A* **2013**, *1*, 3387−3394.

https://doi.org/10.1021/acsomega.2c04060
ACS Omega 2022, 7, 38613−38621